# EXPERIMENTAL CHARACTERIZATION OF DYNAMIC TENSILE STRENGTH IN OFF-AXIS CARBON/EPOXY COMPOSITES

**Norihiko Taniguchi*, Tsuyoshi Nishiwaki*, and Hiroyuki Kawada****
***Institute of sport science, ASICS Corporation**
****Department of mechanical engineering, Waseda University**

**Keywords**: *Impact behavior, Tensile strength, Carbon/epoxy composites, Split Hopkinson bar, Strain rate effect*

***Abstract***

*The tensile strength of unidirectional carbon fiber reinforced plastics under a high strain rate was experimentally characterized. A high-strain-rate test was performed using the tension-type split Hopkinson bar technique with a special fixture for the impact tensile specimen. In order to minimize the extension-shear coupling effect, an oblique tab technique was applied. The experimental results demonstrated that the tensile strength increase with strain rate. The strain rate effect of material principal directions on tensile strength are also investigated by the use of the rosette analysis and the strain transformation equations. It is found that the shear strain rate produces the more significant contribution to strain rate effect on dynamic tensile strength. The experimental results were compared with the tensile strength predicted based on the Hashin-Rotem failure criterion. The results imply that the application limit of this failure criterion exists for the prediction of the tensile strength under the dynamic condition. The fracture behavior translation from static to dynamic must be incorporated for more accurate prediction.*

## 1 Introduction

Carbon/epoxy composites have been recognized for their high performance and good mechanical properties. They have been widely used not only in the aerospace industry but also to manufacture sports gear. In order to design the practical structures of composite material for a variety of sports gear, it is essential that they possess excellent mechanical properties under a dynamic load. Especially, the dynamic tensile strength is one of the most important factors.

A considerable number of studies, which investigate the dynamic tensile behavior of composite materials, have been made. Staab and Gilat [1] investigated the strain rate effect of tensile strength in the case of angle-ply glass/epoxy laminates. Harding and Welsh [2] developed a technique for the impact tensile testing of a unidirectional composite by modifying the split Hopkinson bar (SHB) method. They employed cement to fix the specimen between the input and output bars. Although this method provides a strong grip, it is very inconvenient. Ross et al. [3] proposed a dumbbell-typed specimen with a special specimen holder. However, the disadvantages of this method are that it takes time to machine the specimen and it is difficult to use a plate-like specimen.

In this study, the dynamic tensile strength of off-axis carbon/epoxy composites is experimentally characterized. First, the tension-type split Hopkinson bar apparatus with a specific fixture for impact tensile specimen is proposed. Then, the dependence of strain rate on tensile strength is experimentally investigated. Finally, the discussion associated with the fracture behavior under static and dynamic condition is conducted.

## 2 Experimental method

### 2.1 Tension-type split Hopkinson bar

A high-strain-rate test was performed using a tension-type split Hopkinson bar (SHB) technique (Fig.1). It consists of an input bar with a flange, an output bar, and a cylindrical striker. The data obtained from the SHB method comprise the strain histories of the input and output bars. In the present

study, the strain histories are recorded from the strain gauges at a sampling rate of 1.0 MHz via a DC amplifier. In the SHB system, the specimen stress can be derived from the following equation,

$$\sigma = \frac{AE\varepsilon_t}{A_s} \qquad (1)$$

where $\varepsilon_t$, $E$, $A$, and $A_s$ denote the transmitted strain waves, the bar's Young's modulus, the bar's cross-sectional area, and the specimen's cross-sectional area, respectively. Furthermore, strain of specimen is directly measured from the strain gauge glued on specimen. An important issue in construction of the tension-type SHB is the fixing of the specimen without causing it to slip. In this study, a special fixture for the impact tensile specimen is developed. The fixture design used in this study is illustrated in Fig.1 (b). The bar end has a tapered thread and a slot that is diametrically parallel to the region where the specimen is inserted. A saw-toothed slotted area is machined with precision. A compression ring with a thread, which compensates for the area loss caused by the slot, is mounted at the bar ends to fix the specimen. It was found that this fixing technique could transmit tensile loads of up to 3,000 N as it stands.

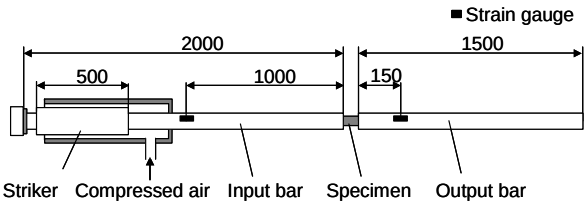


Fig.1(a) Tension-type SHB apparatus constructed in this study

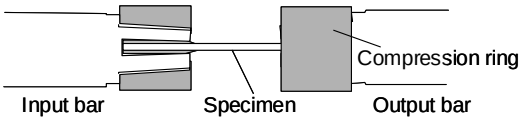


Fig.1(b) A schematic drawing of fixture design in this study

## 2.2 Specimens

The specimens are fabricated by stacking Carbon/epoxy composite. The end tabs were cut from glass/epoxy composite panels and then bonded on the specimens. It is noted for off-axis specimen that the extension-shear coupling resulting from anisotropic behavior is important issue. In order to minimize this effect, specimen with an aspect ratio that is in the range of 12 to 15 is recommended. However, it is practically difficult for a long specimen to achieve the high-strain-rate condition. In this study, the oblique tab [4] is applied. The specimen geometry is shown in Figure 1. The oblique angle $\phi$ is expressed as follows,

$$\cot\phi = -\frac{\bar{S}_{16}}{\bar{S}_{11}} \qquad (2)$$

where $\bar{S}_{ij}$ is the compliance coefficients with respect to the xy coordinate system. The employed oblique angle is shown in Figure 3 as a function of fiber orientation angle for each strain rate. The average oblique angles for the 10º, 15º, 30º, 45º, 60º, and 75º off-axis tensile specimens are 27º, 26º, 38º, 55º, 73º, and 84º, respectively.

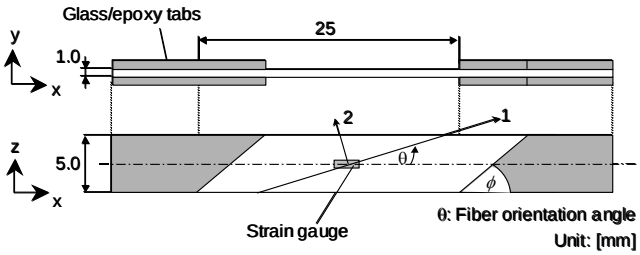


Fig.2 Geometry of off-axis specimen with oblique tab

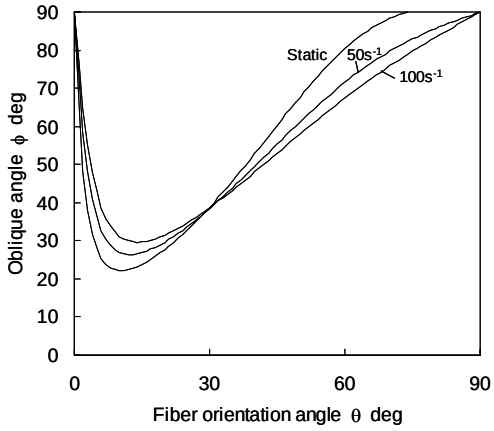


Fig.3 Calculated oblique angle for the static condition, strain rate of 50 $s^{-1}$, and strain rate of 100 $s^{-1}$

## 3 Results

### 3.1 Input, reflect, and output waves

Figure 4 shows the typical example of strain gauge output for 15º specimen. An important assumption in Equation (1) is that the wave propagation effects within the specimen are negligible. In other words, the load $P_i$ between the input bar and specimen may be equivalent to the load $P_o$ between the output bar and specimen (it follows that $\varepsilon_i + \varepsilon_r = \varepsilon_t$ .). Figure 5(a) shows the comparison of load $P_i$ and $P_o$ for 15º specimens. The experimental result shows that the load $P_i$ almost agree with the load $P_o$, except for the initial stage.

Hence, the Equation (1) is applicable in this study; the tensile strength can be determined from the transmitted strain wave. Also, strain and strain rate of specimen are directly measured from the strain gauge glued on specimen as shown in Figure 5(b).

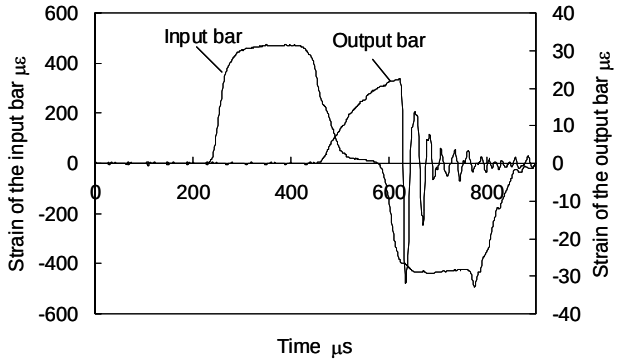


Fig.4 Strain gauge outputs from the input and output bars for the 15º specimen

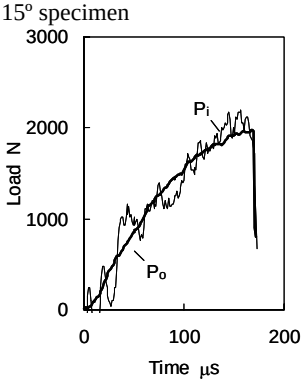


Fig.5 (a) Comparison of load histories of 15º specimen at each face of the bars

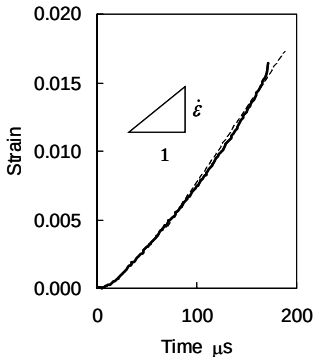


Fig.5 (b) Strain gauge output of 15º off-axis specimen under dynamic loading

### 3.2 Verification of stress uniformity

To measure the tensile strength of off-axis specimen, it is important to achieve a state of uniform stress. In this study, three strain gauges are mounted on 15º off-axis specimen to check the strain distribution under dynamic tensile loading. The strain distribution with rectangular tab is also measured for comparison. Figure 6 (a) and (b) show the comparison of strain between the conventional and oblique tabs. The strain gauge positions and the photograph of fractured specimens are also shown. In Figure 6 (a), the large stress concentration can be observed at gauge position 3, which leads to the premature failure at tabbed area. On the other hand, the strain distribution is almost uniform when oblique tabs are employed (see Figure 6 (b)). Further, the failure position was mainly in the gauge section of specimen. These experimental results indicate that the oblique tab is superior to the conventional tabs for evaluating the dynamic tensile strength of off-axis specimen.

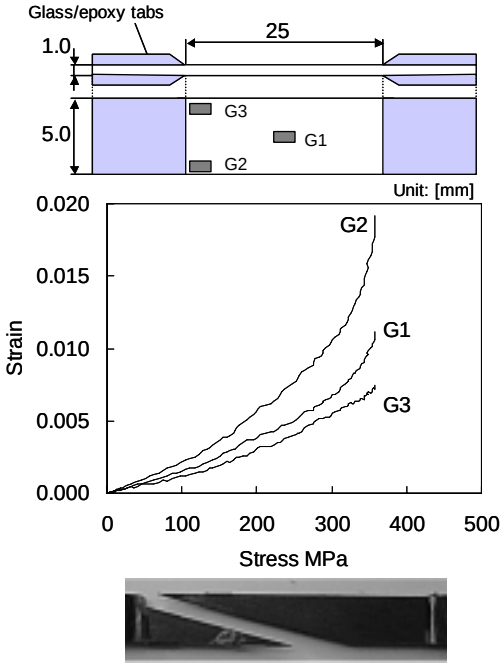


Fig.6 (a) Strain distributions and fracture position of 15° specimen with rectangular tabs

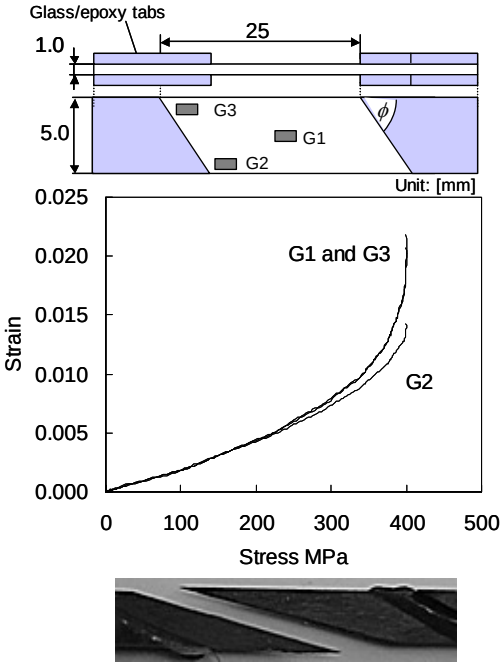


Fig.6 (b) Strain distributions and fracture position of 15° specimen with oblique tabs

### 3.3 Dynamic stress-strain curve

Typical examples of stress-strain curve for 10º, 15º, 30º, 45º, 60º, 75º, and 90º specimen, whose strain rate are =1.04E-04 $s^{-1}$ (static) and 100 $s^{-1}$ are shown in Fig.7 (a) - (d). It is noted that the tensile test of 90º specimens are performed using the rectangular tabs. The two different carbon/epoxy composite systems, the unidirectional T700S/2500

(Toray Industries, Inc.) and TR50S/modified epoxy (Mitsubishi Rayon Co., Ltd.), were tested. It is clear that the strain rate dependency can be confirmed for all specimens; the tensile strength increases with strain rate.

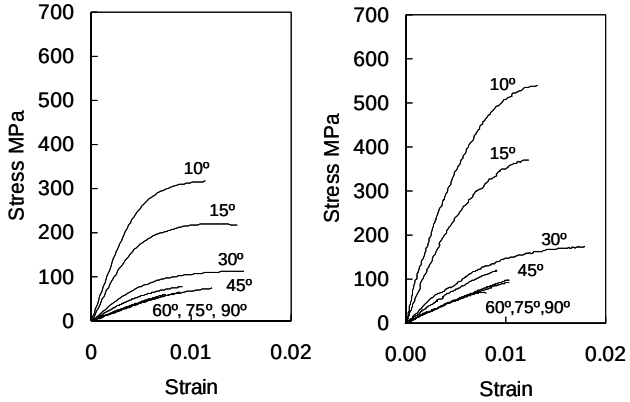


(a) T700S/2500 static (b) T700S/2500 dynamic

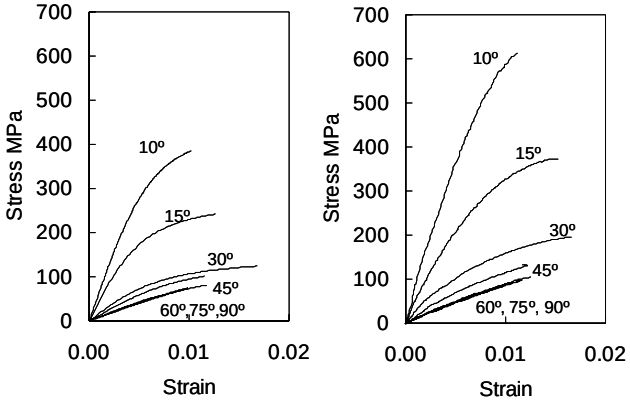


(c) TR50S/modified epoxy static (d) TR50S/modified epoxy dynamic

Fig.7 Stress-strain curves for the 10º, 15º, 30º, 45º, 60º, 75º, and 90º specimens

## 4 Discussion

### 4.1 Dependence of strain rate on tensile strength

The relationship between the strain rate and the tensile strength is shown in Fig.8 (a) and (b) for T700S/2500 and TR50S/modified epoxy, respectively. It is shown that the tensile strengths in the range of 10º-90º specimens increase with strain rate. The summary of tensile strength under static and strain rate of $100s^{-1}$ *is* listed in Table 1. It is confirmed that the higher fiber-orientated specimens, such as 10º and 15º off-axis specimens, produce the more significant contribution to the strain rate dependency. It is also possible to divide the strain rate in the loading direction into each material principal direction, that is, the strain rate in longitudinal, transverse and shear directions. By the application of the rosette analysis and the strain transformation equations as follows, the strain rate effect of material principal directions on tensile strength are investigated

$$\dot{\varepsilon}_1 = \dot{\varepsilon}_x \cos^2\theta + \dot{\varepsilon}_y \sin^2\theta + \dot{\gamma}_{xy} \sin\theta\cos\theta \quad (3)$$

$$\dot{\varepsilon}_2 = \dot{\varepsilon}_x \sin^2\theta + \dot{\varepsilon}_y \cos^2\theta - \dot{\gamma}_{xy} \sin\theta\cos\theta \quad (4)$$

$$\frac{\dot{\gamma}_{12}}{2} = -\dot{\varepsilon}_x \sin\theta\cos\theta + \dot{\varepsilon}_y \sin\theta\cos\theta + \frac{\dot{\gamma}_{xy}}{2}(\cos^2\theta - \sin^2\theta) \quad (5)$$

Figure 9 shows the relationship between fiber orientation angle and strain rate in each material principal direction at strain rate of $100s^{-1}$. At the higher fiber-orientated specimens, it is clear that strain rate in shear direction is much larger than that in longitudinal and transverse direction. On the other hand, at the lower fiber-orientated specimens, strain rate in transverse directions becomes dominant. According to the experimental results of 90º specimens, the transverse strain rate effect on tensile strength is relatively small. This result implies that the shear strain rate makes a great influence on tensile strength in carbon/epoxy composites.

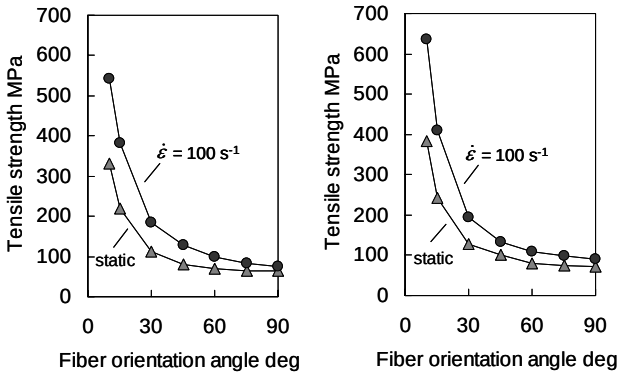


(a) T700S/2500 (b) TR50S/modified epoxy

Fig.8 Comparison of tensile strength between static and strain rate of 100 $s^{-1}$

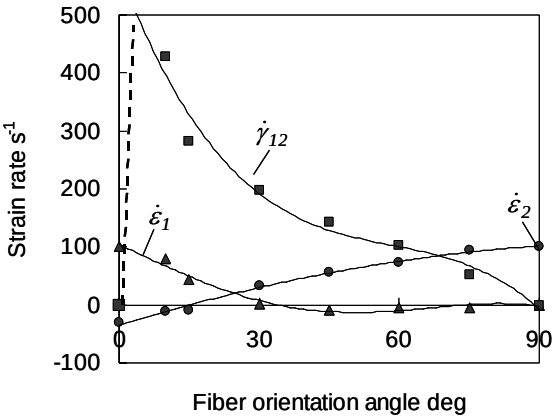


Fig.9 Comparisons of the strain rate in material principal direction under $\dot{\varepsilon} = 100\ s^{-1}$

Table 1 A summary of tensile strength for static and strain rate of $100s^{-1}$

| Fiber orientation angle | T700S/2500 (MPa) | | TR50S/modified epoxy (MPa) | |
|---|---|---|---|---|
| | Static condition | Strain rate: 100 $s^{-1}$ | Static condition | Strain rate: 100 $s^{-1}$ |
| 10º | 330.4 | 541.3 | 382.3 | 635.5 |
| 15º | 218.3 | 382.2 | 243.5 | 409.0 |
| 30º | 113.4 | 183.5 | 127.0 | 194.9 |
| 45º | 80.9 | 128.0 | 100.5 | 134.2 |
| 60º | 70.3 | 98.0 | 79.6 | 109.6 |
| 75º | 65.1 | 84.0 | 74.6 | 97.4 |
| 90º | 63.1 | 74.4 | 72.6 | 91.6 |

### 4.2 Fracture surface observation

Fracture surface observation is carried out by using a scanning electron microscope. The comparison of the fracture surface between static and dynamic (=100 $s^{-1}$) is shown in Fig.10 and Fig.11 for 10º, and 90º specimens. In the static test of T700S/2500 specimen, it is clear that the interfacial fracture can be observed for both specimens. The crack propagates along the interface between the fiber and the matrix. On the other hand, in the dynamic test, crack propagates not only the fiber/matrix interface but also the matrix itself. The region of matrix fracture in off-axis specimen strongly depends on the fiber orientation angle, i.e., fracture surface of 10º off-axis specimens is predominated by the cohesion failure of matrix, while the interfacial debonding is predominant in 90º specimens. In the fracture surface of TR50S/modified epoxy, however, there are no significant differences between static and dynamic conditions. It can be said without difficulty that the increase of tensile strength with strain rate is primarily due to the viscoelasticity of the matrix. Furthermore, these results show that the fracture behavior is an important factor for characterizing the strain rate dependency of tensile strength.

### 4.3 Discussion about failure criterion

In order to predict the failure criterion under a high-strain-rate condition, the Hashin-Rotem failure criterion [5] should be discussed. This failure criterion is applied for prediction of the fiber

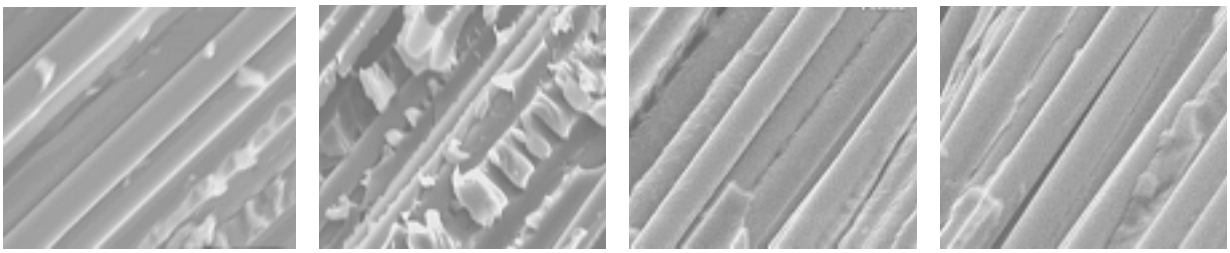

10º specimen (static) 10º specimen (dynamic) 90º specimen (static) 90º specimen (dynamic)

Fig.10 Comparisons of fracture surface between static and dynamic conditions for 10º, and 90º specimens (T700S/2500)

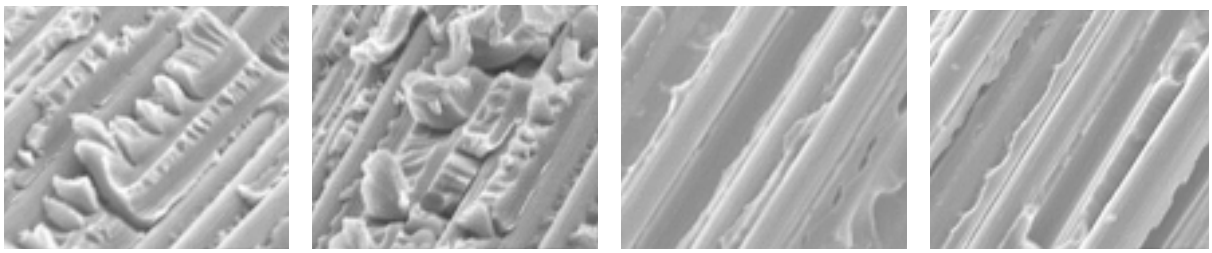

10º specimen (static) 10º specimen (dynamic) 90º specimen (static) 90º specimen (dynamic)

Fig.11 Comparisons of fracture surface between static and dynamic conditions for 10º, and 90º specimens (TR50S/modified epoxy)

breakage and matrix cracking. For the fiber breakage, it is defined as follows,

$$\sigma_{11} \geq X \qquad (6),$$

where $X$ is the longitudinal strength.
For the matrix or interfacial dominated failures, the failure criterion is given by

$$\frac{\sigma_2^{\,2}}{Y^2} + \frac{\tau_{12}^{\,2}}{S^2} = 1 \qquad (7),$$

where $Y$ and $S$ indicate the strength in transverse and shear direction for each strain rate, respectively.

Figure 12 (a) and (b) show the failure envelope predictions for the static and dynamic strain rates. As can be seen in TR50S/modified epoxy composite, the model predictions are in very good agreement with the experiment, suggesting that Hashin-Rotem failure criterion is valid for predicting the rate-dependent tensile strength. Also, it characterizes well the tensile strength of T700S/2500 composite at static condition. However, the model predictions of T700S/2500 at the strain rate of 100 $s^{-1}$ are relatively in poor agreement with the experiment. This disagreement is mainly caused by the fracture behavior translation from static to dynamic conditions. For accurate prediction of dynamic tensile strength of carbon/epoxy composites, this fracture behavior translation must be incorporated.

## 5 Concluding remarks

In this study, tensile strength of unidirectional carbon/epoxy composites is characterized. A high-strain-rate test was performed using the tension-type split Hopkinson bar technique with a special fixture for the impact tensile specimen. It is experimentally found that an oblique tab is applicable to measure the dynamic tensile strength for off-axis specimen. The two different carbon/epoxy composite systems, the unidirectional T700S/2500 and TR50S/modified-epoxy, are tested at the static and dynamic conditions. Experimental results show that both tensile strength increases with strain rate, while the fracture behaviors are quite different. Further, the higher fiber-orientated specimens produce the more significant contribution to the tensile strength. By the use of the rosette analysis and the strain transformation equations, it is experimentally found that the shear strain rate produces the more significant contribution to dynamic tensile strength. Hashin-Rotem failure criterion is discussed as a rate-dependent failure criterion. The results imply that the application limit of this failure criterion exists for the prediction of the tensile strength under the dynamic condition. The fracture behavior translation from static to dynamic must be incorporated for more accurate prediction.

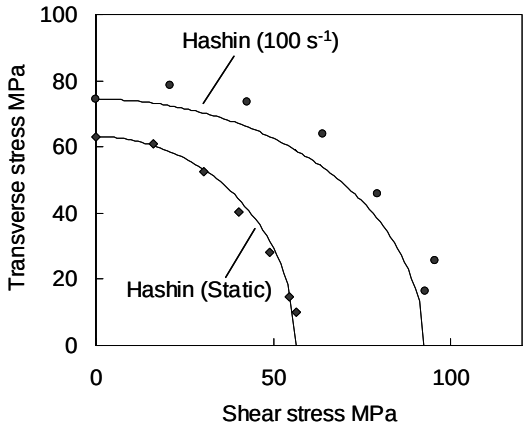


Fig.14 (a) Comparison of the experimental and predicted tensile strength at the static condition, and strain rate of 100 $s^{-1}$ (T700S/2500)

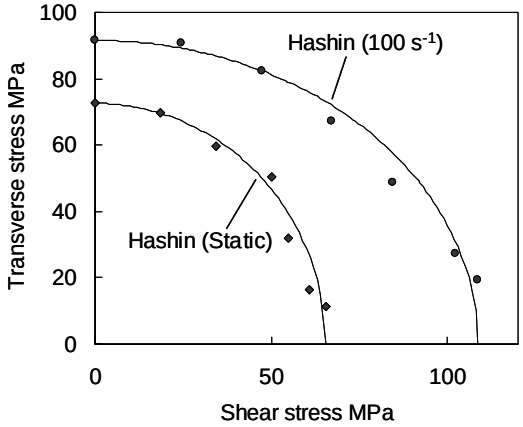


Fig.14 (b) Comparison of the experimental and predicted tensile strength at the static condition, and strain rate of 100 $s^{-1}$ (TR50S/modified epoxy)

## References

[1] Staab, G.H. and Gilat, A., “High strain rate response of angle-ply glass/epoxy laminates”, Jour. Comp. Mater., vol.29, No.10, pp.1308–1320, 1995

[2] Harding, J. and Welsh, L.M., “A tensile testing technique for fibre-reinforced composites at impact rates of strain”, Jour. Mater. Sci., vol.18, pp.1810–1826, 1983

[3] Ross, C.A., Cook, W.H. and Wilson, L.L., “Dynamic tensile tests of composite materials using a split-Hopkinson pressure bar”, Exp. Tech., November, pp.30–33, 1984

[4] Sun, C.T. and Chung, I., “An oblique end-tab design for testing off-axis composite specimens”, Composites, vol.24, No.8, pp.619–623, 1993

[5] Hashin, Z., Failure criteria for unidirectional fiber composites, J. App. Mech., 1980; 47: 329-334